Available online at www.sciencedirect.com
ScienceDirect
Materials and Design 29 (2008) 1600–1608
Materials & Design
www.elsevier.com/locate/matdes

Influence of matrix structure on the fatigue properties of an alloyed ductile iron

Gülcan Toktaş *, Alaaddin Toktaş, Mustafa Tayanç

Department of Mechanical Engineering, Balıkesir University, 10145 Balıkesir, Turkey

Received 21 May 2007; accepted 25 October 2007
Available online 30 October 2007

Abstract

Rotary bending fatigue tests were conducted on ductile iron containing 1.25 wt% nickel, 1.03 wt% copper and 0.18 wt% molybdenum with various matrix structures. Several heat treatments were applied to obtain ferritic, pearlitic/ferritic, pearlitic, tempered martensitic, lower and upper ausferritic structures in the matrix of a pearlitic as-cast alloyed ductile iron. The tensile properties (ultimate tensile strength, 0.2% yield strength and percent elongation), the hardness and the microstructures of the matrixes were also investigated in addition to fatigue properties. Fractured surfaces of the fatigue specimens were examined by the scanning electron microscope. The results showed that the lowest hardness, tensile and fatigue properties were obtained for the ferritic structure and the values of these properties seemed to increase with rising pearlite content in the matrix. While the lower ausferritic structure had the highest fatigue strength, the upper ausferritic one showed low fatigue and tensile properties due to the formation of the second reaction during the austempering process.

Keywords: Ferrous metals and alloys; Heat treatments; Fatigue

1. Introduction

Ductile iron has several engineering and manufacturing advantages when compared with cast steels. These include an excellent damping capacity, better wear resistance, 20–40% lower manufacturing cost and lower volume shrinkage during solidification [1]. The combination of good mechanical properties and casting abilities of ductile cast iron makes its usage successful in structural applications especially in the automotive industry [2]. Gears, camshafts, connecting roads, crankshafts, front wheel spindle supports and truck axles are some of the application areas of ductile iron in the automotive industry [1,3–5]. As known these machine parts and many of others are often subjected to fluctuating loads in service. For example; connecting roads are pushed and pulled in piston engines. Crankshafts are generally subjected to torsional stress and bending stress due to self-weight or weight of components or possible misalignment between journal bearings. In all such cases the metal is liable to fracture by fatigue which is the most common of all causes of engineering failure [5,6]. The most characteristic feature of fatigue fracture is that even with the most ductile materials, failure takes place without revealing any plastic deformation, and generally when the part has been stressed repeatedly below the elastic limit. This feature of fatigue fracture necessitates the availability of data on fatigue strength of material for design purposes. Some of the important variables that influence the fatigue behavior of any material are stress concentration, corrosion, operating temperature, stress ratio, metallurgical structure and residual stresses [7].

A large scatter in fatigue strength of ductile irons indicates there are many variables on which the fatigue strength is dependent. These variables that influence the fatigue properties of ductile iron are graphite shape, graphite size, nonmetallic inclusions, matrix hardness and struc-

* Corresponding author. Tel.: +90 266 612 11 94; fax: +90 266 612 12 57.
E-mail address: gzeytin@balikesir.edu.tr (G. Toktaş).

0261-3069/$ - see front matter © 2007 Elsevier Ltd. All rights reserved.
doi:10.1016/j.matdes.2007.10.001

ture, specimen size, surface condition, surface degradation such as corrosion and the type of loading [5,7].

The fatigue properties of ductile cast iron have been studied by many investigators. Janowak et al. [8] have shown that composite matrix microhardness (CMMH) correlates well with fatigue endurance limit (FEL) of commercial ductile iron castings and FEL of ductile iron is increased with increased CMMH, pearlite content, cleanliness, soundness, nodule count, and optimized chemical composition. Research by Faubert et al. [9] on fatigue properties in as-cast and austempered specimens showed that fatigue strength at 20×10^6 cycles in heavy-section castings was higher for the austempered specimens than for the as-cast pearlitic specimens. Another work by these authors [10] showed that the fatigue strength had a small sensitivity to position within the casting, only 15% difference from the best to the worst conditions in fatigue was mentioned. Tayanç et al. [11] studied the rotary bending fatigue properties of unalloyed ductile iron which were austempered at different austempering temperatures and times. They reported that feathery-type ferrite characteristics of ausferritic microstructure resulted in higher fatigue strength than acicular ferrite characteristics of ausferritic microstructure. Krishnaraj et al. [7] investigated the fatigue behavior of ductile iron with different matrix microstructures. They reported that among ductile irons with different matrix structures, the one with bainitic matrix possessed the highest fatigue limit. Bahmani et al. [3] investigated the relationship between fatigue strength and microstructure in an austempered Cu–Ni–Mn–Mo alloyed ductile iron. The correlation between fatigue strength and austempered microstructure was evaluated depending on the amount of retained austenite, X_γ, and its carbon content, C_γ. They concluded that the highest fatigue strength was observed in an ausferritic structure with a high $X_\gamma C_\gamma$ value.

The purpose of the current work is to investigate the influence of matrix structure on the fatigue behavior of an alloyed ductile iron. Fracture surfaces were also observed by scanning electron microscope in order to identify the fracture morphologies of the matrix structures.

2. Experimental procedures

2.1. Material

The alloyed ductile iron used in the present work was produced in a medium frequency induction furnace of 350 kg capacity. The foundry practice followed is given in the previous work [12]. The chemical composition of the produced ductile iron is presented in Table 1. The matrix structure and the nodule appearance of the as-cast material are shown in Fig. 1. The microstructure of the as-cast ductile iron showed a bull's eye structure with ferrite surrounding the graphite nodules in a pearlitic matrix.

2.2. Heat treatments

In order to investigate the effect of matrix structure on the fatigue behavior of ductile iron, six various types of heat treatments were applied. The details of the heat treatments are given in Table 2. According to the applied heat treatments ferritic, pearlitic/ferritic, pearlitic, tempered martensitic, lower and upper ausferritic structures were obtained and these structures are defined as F, P/F, P, TM, LA and UA throughout the paper, respectively. Usually, ADI (austempered ductile iron) material is difficult to machine after heat treatment, so all the test specimens were fabricated prior to heat treatment.

Table 1
Chemical composition of the material (wt%)

C	3.73
Si	2.55
Mn	0.30
P	0.045
S	0.023
Mg	0.044
Cu	1.03
Ni	1.25
Mo	0.18
Cr	0.032

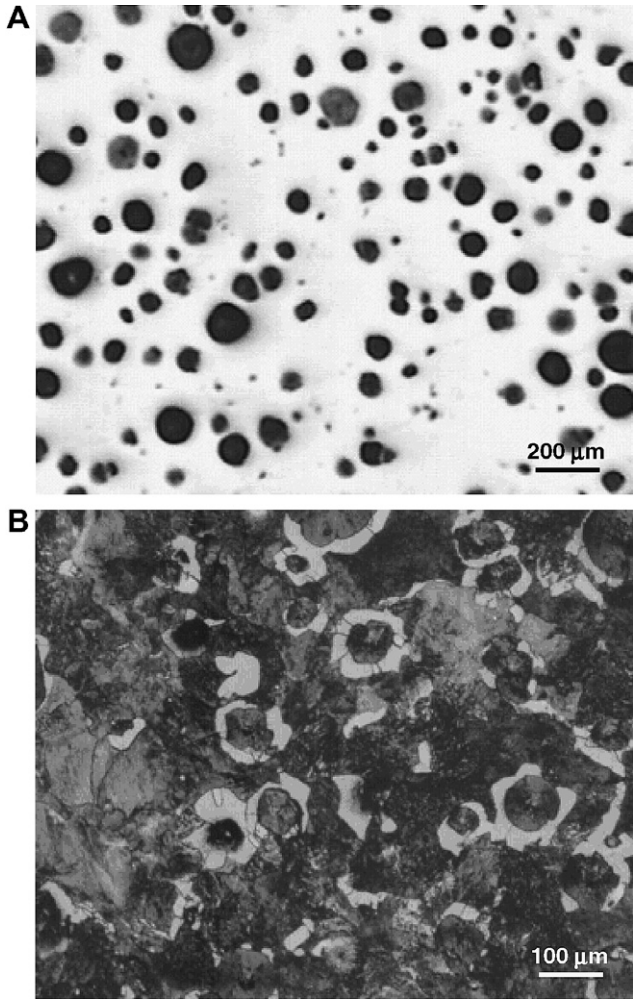

Fig. 1. Microstructure of the material in as-cast condition: (A) unetched and (B) etched.

2.3. Fatigue testing

Fatigue tests were carried out in a rotary bending fatigue testing machine at a frequency of 3000 rpm (50 Hz) with a reversed cycle of stress (R= minimum stress/maximum stress = −1). Fatigue specimens were

Table 2
Sample identification and heat treatment parameters

Sample identification	Austenitizing temperature (°C)/time (h), T_γ/t_γ	Tempering and/or cooling conditions
Ferritic (F)	925/7	925–500 °C → furnace cooling 500–RT → air cooling
Pearlitic/ferritic (P/F)	900/1	Cooling to 660 °C with 2.4 °C/min, then air cooling
Pearlitic (P)	900/1	Cooling to 650 °C with 5 °C/min, then air cooling
Tempered martensitic (TM)	900/1	Tempering at 400 °C for 1 h, then air cooling
Lower ausferritic (LA)	900/1	Austempering at 300 °C for 1 h, then air cooling
Upper ausferritic (UA)	900/1	Austempering at 365 °C for 1 h, then air cooling

machined with the dimensions of 10 mm diameter and 100 mm length prior to heat treatment. The tests were run to failure or to 10^7 cycles at which specimen was considered to be a runout. Sixteen specimens for each matrix structure were tested at sufficient stress levels to obtain reliable S–N curves and fatigue limits. The bending stress was calculated by using the following equation:

$$\sigma_g = \frac{P \cdot l \cdot 32}{\pi \cdot d^3}, \quad (1)$$

where σ_g is the stress amplitude (MPa), P is the applied load (N), l is the length of moment (constant at 80 mm) and d is the diameter of the fatigue specimen (mm).

A smooth curve was drawn through the data points rather than a straight line, as it fitted the data points better. Arrows on data points indicate that the samples did not fail even after 10^7 cycles. The highest stress at which the samples endured 10^7 cycles was taken as the fatigue strength. The fatigue ratio for each matrix was calculated as the fatigue strength divided by the ultimate tensile strength.

2.4. Microstructural and fractographic analysis

An image analyzing system was applied to evaluate the graphite structure such as nodule counts, nodule diameter, nodularity and area fraction of nodules. These observations were carried out by Buehler Omnimet imager analyzer and by calculating the average of six observed areas on 20 mm diameter polished specimens for each matrix structure. Metallographic examinations were done by applying standard methods of specimen preparation and etching by 2% nital. Postfailure fractographic analysis was performed by scanning electron microscopy (SEM). Fracture surfaces of the broken fatigue specimens were examined to determine the failure mechanism of matrix structures in ductile iron.

2.5. Other mechanical properties

Brinell hardness tests were applied on ground and polished surfaces by applying 187.5 kg load with a 2.5 mm diameter steel ball indenter and by calculating the average of five values for each matrix. Tensile testing of the heat treated irons was performed on a 25 ton Shimadzu testing machine according to TS 138 standard [13] at a constant engineering strain rate of 4×10^{-4} s^{-1}. Six specimens were tested for each matrix and 0.2% yield and tensile strengths and percent elongation were calculated by averaging six values. The geometry of the tensile specimen is given in Fig. 2.

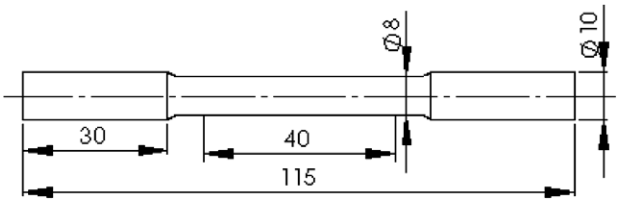

Fig. 2. Geometry of tensile specimen.

3. Results and discussion

3.1. Microstructure and monotonic mechanical properties

Fig. 3A–F displays the microstructures and Table 3 shows the nodule characteristics of the matrixes obtained by the applied heat treatments. Ferritic, pearlitic/ferritic, pearlitic, tempered martensitic, lower and upper ausferritic matrix structures can be seen clearly from Fig. 3A–F, respectively. While austempering at 300 °C exhibited the needle shaped acicular bainitic ferrit (dark areas), the microstructure treated at 365 °C showed feathery coarse bainitic ferrit with more blocky austenite (white areas) as seen in Fig. 3E and F, respectively. The tensile properties (0.2% proof strength, ultimate tensile strength and percent elongation) and the hardness values of the mentioned structures are given in Table 4. The lowest hardness and tensile properties (0.2% proof strength and ultimate tensile strength) are obtained for the F structure. It is seen that the values of these properties are increased with the rising pearlite content of the matrix structure (Fig. 3A–C and Table 4). As it is well known that the fast cooling rate increases the pearlite content and also decreases the lamellar spacing of the pearlitic structure and this causes to increase the hardness of the material [14]. The TM structure has displayed the highest 0.2% proof and ultimate tensile strengths and the second high hardness value of all the structures as 934 MPa, 1147 MPa and 309 HB, respectively. The elongation value of this structure is the second lowest of all the studied matrixes. As for most materials, elongation is inversely proportional to hardness.

The LA structure showed the best combination of tensile properties and hardness. The literature review [15–17] shows that lower austempering temperatures give the material a higher strength and a lower ductility because of a large volume fraction of acicular ferrite and lower amounts of stabilized austenite in the microstructure. In the present study the lower austempering temperature (300 °C) produced higher strength in agreement with the literature, but also higher ductility contrary to the literature. The higher austempering temperature (365 °C) showed the

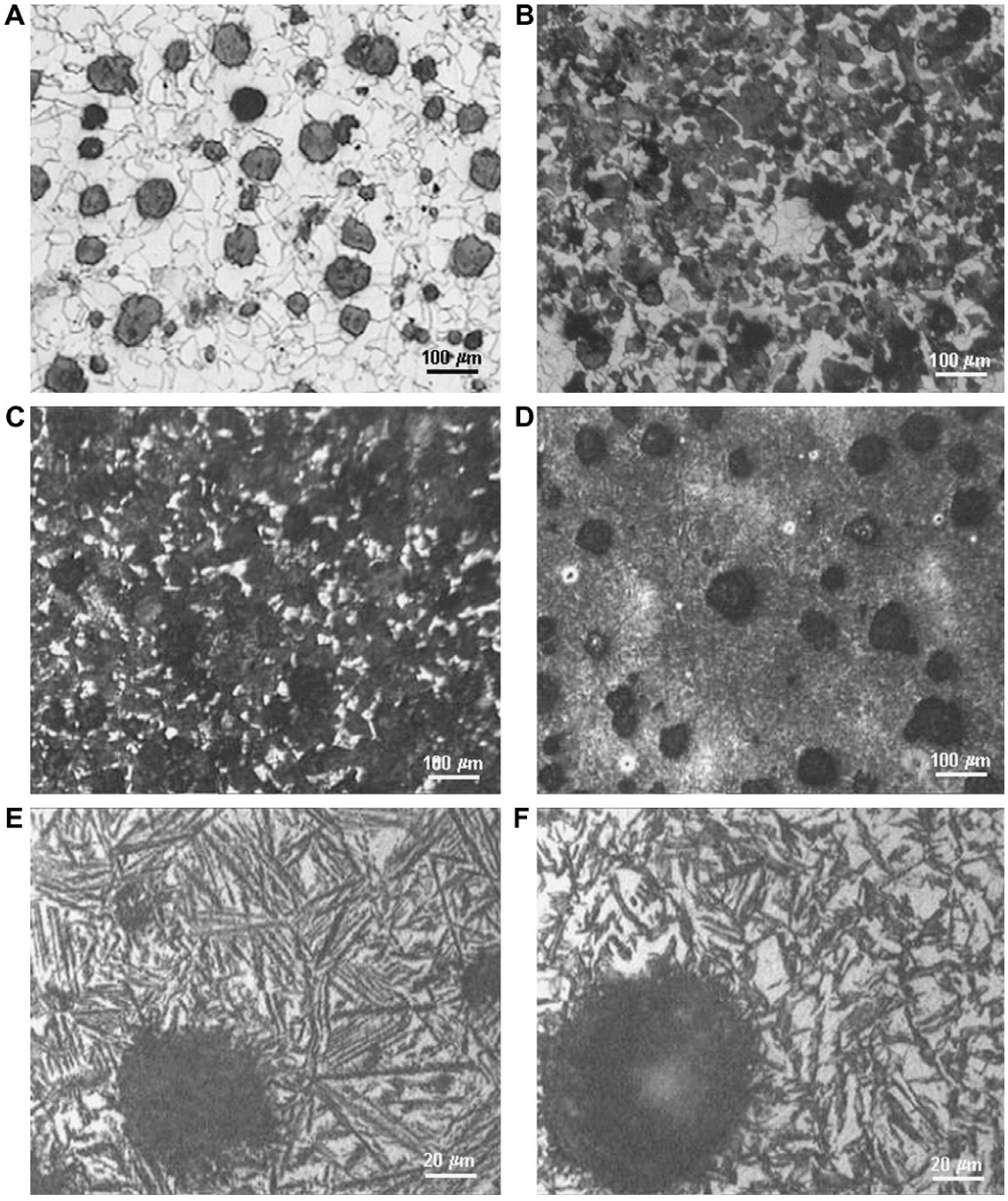

Fig. 3. Matrix structures obtained by heat treatments: (A) ferritic, (B) pearlitic/ferritic, (C) pearlitic, (D) tempered martensitic, (E) lower and (F) upper ausferritic.

Table 3
Nodule characteristics of matrix structures

Matrix structure	Nodule count (mm^{-2})	Area fraction of nodule (%)	Nodule diameter (μm)	Nodularity (%)
F	135.6	9.1	32	95.9
P/F	119.3	10.8	37	95.5
P	146.4	9.4	30	92.4
TM	118.8	9.2	32	92.6
LA	100.6	8.8	34	95.2
UA	155.3	9.6	29	96.3

Table 4
Tensile and hardness properties of matrix structures

Matrix structure	0.2% Yield strength (MPa)	Ultimate tensile strength (MPa)	Elongation (%)	Hardness (HB)
F	345	502	10.94	175
P/F	470	635	8.37	226
P	490	682	7.1	255
TM	934	1147	5.32	309
LA	704	1025	13.12	277
UA	489	625	3.96	329

highest hardness and the lowest percent elongation. This contradiction can be explained by stage II or by the second reaction that is formed during austempering process at 365 °C. If the casting is held at the austempering temperature for too long or at the high austempering temperature for a certain time, a second reaction takes place and high-carbon austenite can decompose further into ferrite and carbide. In this case, as the structure contains carbides, the material becomes brittle and this causes to the degradation of mechanical properties.

According to the literature [18–21], second reaction takes place at higher austempering temperatures than the temperature used in the present study. The processing window that is known as the time between the completion of the first reaction and the onset of the second reaction depends on austempering temperature, austempering time and alloying elements of the iron. While Ni, Cu and Mo alloying elements widen the processing window, Cr and Mn narrow it [22–25]. These elements can display various effects when added individually or in combination. Bosnjak et al. [26] studied the effect of Ni and Mo alloying additions when added individually or in combination. They explained that the closure of the processing window occured at a relatively low austempering temperature (300 °C) in complex Ni–Mo alloyed iron. So, it can be easily said that austempering at 365 °C caused to exceed the processing window in this study and resulted in the formation of the second reaction where carbon enriched austenite decomposes into ferrite and carbide. On the other hand, the formation of carbide can cause to decrease the carbon content of the matrix and makes it easy to form brittle martensite phase during the cooling process from austempering temperature to room temperature. This may be the second reason for high hardness and low elongation in the upper ausferritic structure (austempered at 365 °C).

3.2. Fatigue properties

Results of the rotary bending fatigue *S–N* curves for all matrix structures are shown in Fig. 4A–F. The estimated fatigue strengths and fatigue ratios are also given in Table 5. The lowest fatigue strength is obtained as 170 MPa for the F structure. Fatigue strengths of P/F and P structures are 225 MPa and 235 MPa, respectively. When the pearlite content is increased in the microstructure of ductile iron, considerable increases (32–38%) are observed in fatigue strengths. Similar result is also reported in the literature [7,27]. The fatigue strength is increased with the increasing matrix hardness and static strength (Tables 4 and 5).

Fatigue strength of TM structured ductile iron is estimated higher (255 MPa) than the fatigue strengths of F, P and P/F structures. Although the static strength and hardness values of the tempered structure are much higher than the same properties of F–P structures, the fatigue strength of TM structure is not as much as expected. Krishnaraj et al. [7] reported the fatigue strength of the tempered martensitic ductile iron as 360 MPa, rather higher than the ferritic ductile iron (240 MPa) containing 3.6%C, 1.82%Si and 0.39%Mn. They austenitized the ductile iron at 960 °C for 2 h and tempered at 550 °C for 2 h. The reasons of the relatively low fatigue strength of the tempered structure in this study may be the secondary graphite precipitation in the matrix during the tempering, the effects of the alloying elements, tempering conditions and the differences in fatigue test conditions (dimensions of fatigue specimens, frequency, type of the applied load, etc.). Tempering ductile iron in the range from 425 °C to 600 °C is a two-staged process. The first involves the precipitation of carbides similar to the process in steels. The second stage involves the nucleation and the growth of small, secondary graphite nodules at the expense of carbides. This results in a decrease in hardness, the magnitude of which depends upon alloy content, initial hardness and tempering time. The drop in hardness accompanying secondary graphitization produces a corresponding reduction in tensile and fatigue strength as well [28].

The LA structured ductile iron showed the maximum fatigue strength of all the matrix structures. Under the rotary bending conditions, the outer surface of the specimen is subjected to the maximum applied stress magnitude when the neutral axis of specimen is not stressed at all. Therefore, fatigue cracks start at or near the surfaces of specimens [29]. Austempered ductile irons are strain hardenable in cyclic loading because of the retained austenite (high-carbon austenite) phase in the microstructure. Austenite undergoes strain hardening with high plastic deformation at the crack tip. In addition, stress-induced martensitic transformation of austenite occurs locally in the plastic zone ahead of the crack so as to relax the stress concentration at the crack tip. The accompanying volume change also encourages plastically induced crack closure to occur, reducing the fatigue crack growth rate and increasing fracture toughness [7,18,29]. These two factors explain why the austempered ductile irons have higher fatigue strengths than the conventional ductile irons. By the way, it is reported in the literature [4,18] that the fatigue strength of austempered ductile iron is not proportional to the tensile strength and hardness, but is related to toughness and the amount of the retained austenite. Fatigue strength of ADI increases by not only the volume fraction of the retained austenite, but also by the amount of carbon in austenite. Because the interstitial carbon which is present in retained austenite in large amounts induces strain ageing [18].

Bahmani et al. [3] austempered the alloyed ductile iron containing 3.5%C, 2.6%Si, 0.48%Cu, 0.96%Ni, 0.27%Mo and 0.25%Mn in various austempering conditions and investigated the rotary bending fatigue strengths of the austempered ductile iron. They reported that maximum fatigue strength was obtained for the austempered structure possessing maximum ductility and large amount of retained austenite.

The fatigue strength of the UA structure is estimated as 220 MPa (Table 5), approximately 24% lower than the fati-

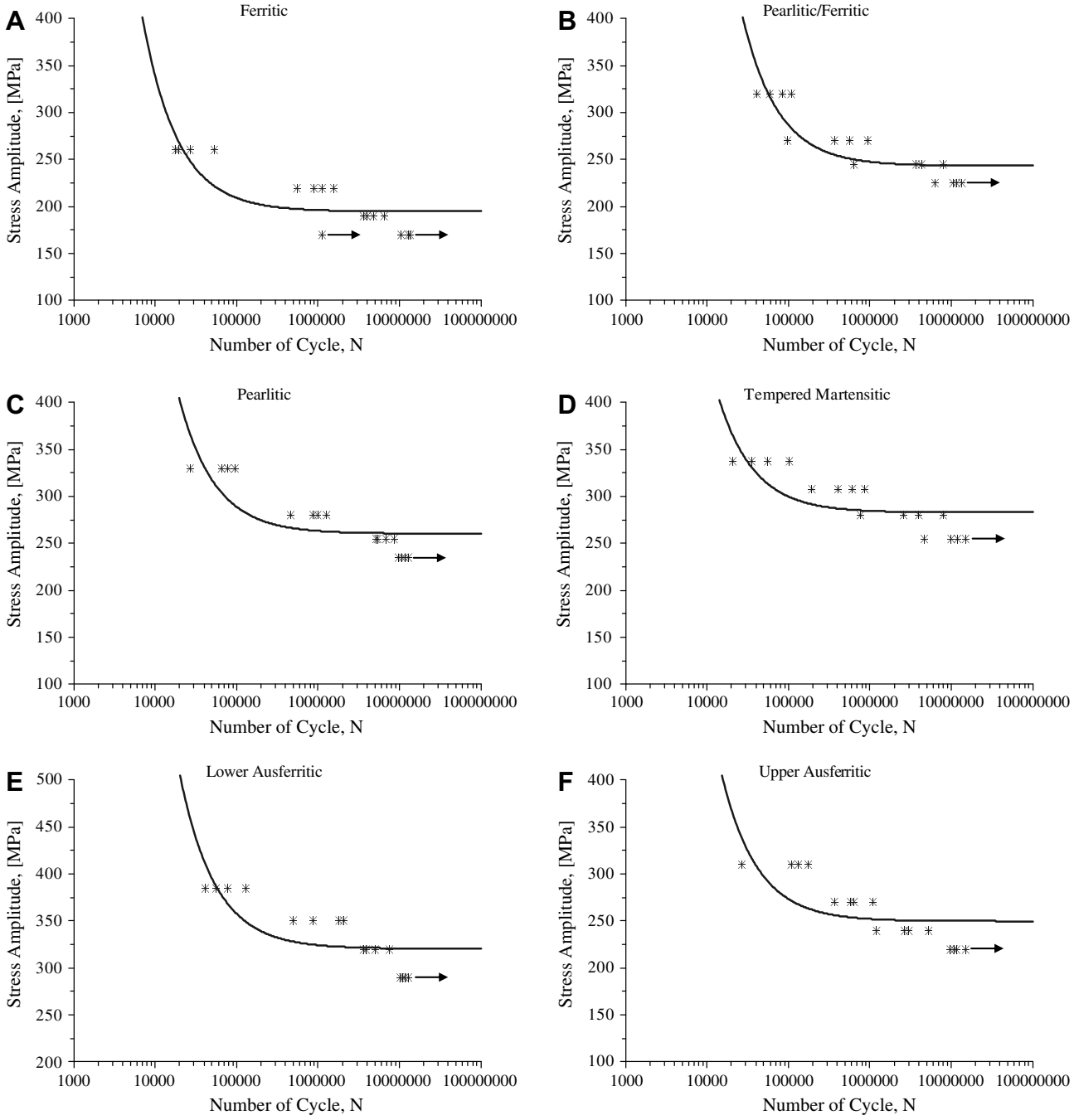

Fig. 4. *S–N* curve of (A) ferritic, (B) pearlitic/ferritic, (C) pearlitic, (D) tempered martensitic, (E) lower and (F) upper ausferritic matrix structures.

Table 5
Estimated fatigue strengths and fatigue ratios of the matrix structures

Matrix structure	Fatigue strength at 10^7 cycles (MPa)	Fatigue ratio σ_f/σ_{uts}
F	170	0.338
P/F	225	0.354
P	235	0.344
TM	255	0.222
LA	290	0.282
UA	220	0.352

gue strength of the LA structure. This result is consistent with the other mechanical properties of the UA structure. While the percent elongation and tensile strength of the UA structure is low, the hardness value is the highest level. These bad mechanical properties are the result of the carbide precipitation in the matrix during austempering by the second reaction. The reason of the low fatigue strength in a carbidic structure can be explained by two important factors. Firstly, carbon content of austenite decreases by the carbide precipitation, which causes to increase the martensite start temperature and it becomes easy to form mar-

tensite in the structure after austempering. Secondly, the shape and the distribution of carbides increase stress concentration in the matrix and can create the notch effect.

Lin and Wei [4] studied the high-cycle fatigue (HCF) properties of a number of different grades of austempered ductile irons. They introduced the following empirical equation to correlate the fatigue limit of ADI with the impact toughness value and mean nodule diameter.

$$S_e = 371.54 \cdot I^{0.31} \cdot d^{-0.40} \quad (r^2 = 0.91) \tag{2}$$

S_e is the fatigue limit (MPa), I is the impact toughness (J), and d is the mean nodule diameter (μm).

The impact toughness values of LA and UA structures at room temperature were reported in the previous study [12] as 99 J and 39.5 J, respectively. When the mean nodule diameters (Table 3) and the impact toughnesses of these structures are put in the above equation, 377 MPa and 302 MPa fatigue strengths are obtained for the LA and UA structures, respectively. The difference between these empirical values is approximately 75 MPa and it is nearly the same for the experimental difference of 70 MPa

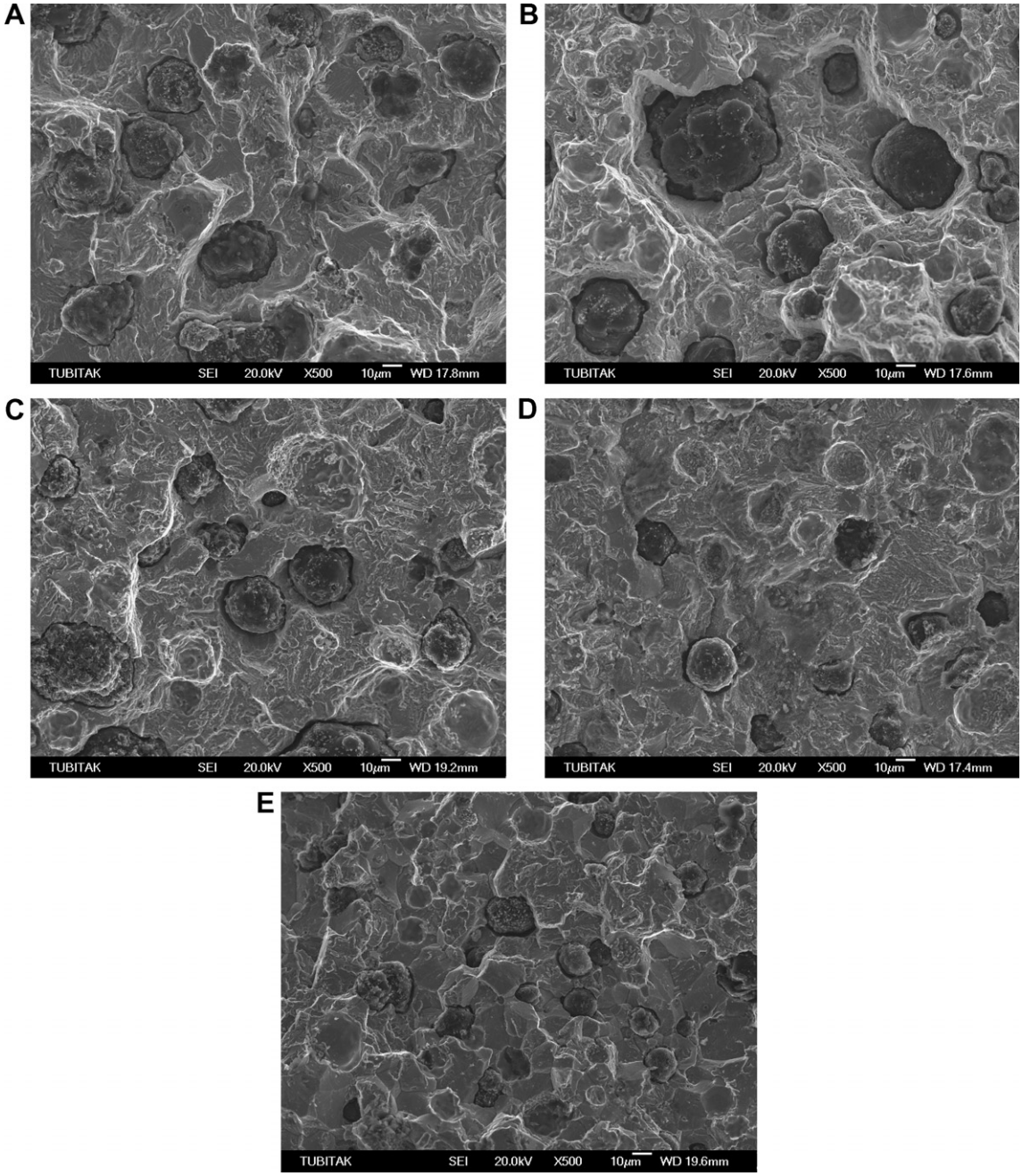

Fig. 5. SEM fractographs of (A) ferritic, (B) pearlitic, (C) tempered martensitic, (D) lower and (E) upper ausferritic matrix structures.

(290 MPa for LA and 220 MPa for UA) in this study. However, the experimental fatigue strengths of LA and UA structures are respectively 23% and 27% lower than the empirical fatigue strengths.

Generally, for all the matrix structures the fatigue strengths were obtained low according to the literature [1,4,7,27,29]. There may be several reasons of the relative low fatigue strengths in the present study. These may be the segregation effect of the alloying elements (especially Mo and Mn), the dimension of the fatigue specimen, the surface quality of the fatigue specimen, the type of the applied stress and other experimental conditions. One of the most important factors of the low fatigue strength is the surface quality of the specimen. As known, fatigue cracks usually form on the surfaces. After heat treatment, no surface preparation was applied to the test specimens in the present study.

Fatigue strengths increased in the order of F, UA, P/F, P, TM and LA microstructures. Similar result is also reported in the literature [7] except for the UA structure that carbide precipitation took place in the microstructure by the second reaction. No correlation between the fatigue ratios and the matrix structures is seen (Table 5). The lowest fatigue ratio is estimated for the TM structure. Literature [27] reports that for ductile irons with a mixed-matrix microstructure, the fatigue ratio varies with the amount of the different constituents, and a general value cannot be defined with confidence. Tempered martensitic and ausferritic structures may contain more than two constituents in their microstructures.

3.3. Fractography

SEM micrographs of fracture surfaces of the fatigued specimens are shown in Fig. 5A–E. Generally all the matrix structures show brittle type of fracture. Besides this, some differences between the micrographs of the matrix structures can also be seen clearly. For example, the fractography of the TM structure is more brittle than the F, P and LA structures, existing no trace of ductile fracture. This result is in a good agreement with the experimental results. The hardness value of this structure is higher than the F, P and LA structures. The fractographic image of the LA structure (Fig. 5D) shows that the striation and quasi-cleavage feature is the dominant fracture mechanism. As shown in Fig. 5E, the fracture surface of UA exhibited the transgranular cleavage type of fracture in convenience with the high hardness, low fatigue and tensile values of this matrix due to the carbide formation in the microstructure by the second reaction.

Fatigue crack initiation in ductile iron is essentially instantaneous, and generally occurs at the graphite nodule/matrix interface. This is due to the weak interface bond and low elastic modulus of graphite. However, crack initiation may also occur at casting imperfections such as non metallic inclusions, large microshrinkage pores and irregularly shaped graphite [11,30,31]. Decohesion of nodules and microcracks around the nodules are also seen in all micrographs.

4. Conclusion

Increasing the pearlite content in the matrix causes to increase the fatigue strength as well as the yield, ultimate tensile strengths and hardness values of ductile iron. The lower ausferritic matrix has the highest fatigue strength among ductile irons with different matrix structures because of the retained austenite in the microstructure. This structure has also the best combination of tensile and hardness properties. Austempering at 365 °C results in carbide precipitation in this alloyed ductile iron by the second reaction. This reaction causes to reduce the mechanical properties including fatigue and tensile and to increase the embrittlement which causes a transgranular type of fracture in fatigue for the UA structure. Fatigue strengths increased in the order of F, UA, P/F, P, TM and LA structures.

Acknowledgements

The authors would like to express their most sincere gratitude and appreciation to the Turkish Land Forces 6th Maintenance Central Commandership and Prof. Dr. Ali Bayram from Uludağ University for their valuable help and cooperation. This research was partially supported by the Research Project Fund of Balıkesir University.

References

[1] Kim JH, Kim MG. Influence of microstructure on fatigue limit of high strength ductile irons. Key Eng Mater 2000;183–187:933–8.
[2] Guillemer-Neel C, Bobet V, Clavel M. Cyclic deformation behaviour and Bauschinger effect in ductile cast iron. Mater Sci Eng A 1999;272:431–42.
[3] Bahmani M, Elliott R, Varahram N. The relationship between fatigue an austempered Cu–Ni–Mn–Mo alloyed ductile iron. J Mater Sci 1997;32:5383–8.
[4] Lin CK, Wei JY. High-cycle fatigue of austempered ductile irons in various-sized Y-block casting. Mater Trans 1997;38:682–91.
[5] Asi O. Failure analysis of a crankshaft made from ductile cast iron. Eng Failure Anal 2006;13:1260–7.
[6] Cottrell A. An introduction to metallurgy. 2nd ed. London: ELBS; 1975.
[7] Krishnaraj D, Rao KV, Seshan S. Influence of matrix structure on the fatigue behavior of ductile iron. AFS Trans 1989;97:345–50.
[8] Janowak JF, Alagarsamy A, Venugopalan D. Fatigue strength of commercial ductile irons. AFS Trans 1990;123:511–8.
[9] Faubert GP, Moore DJ, Rundman KB. Heavy-section ADI: fatigue properties in as-cast and austempered specimens. AFS Trans 1990;166:759–64.
[10] Faubert GP, Moore DJ, Rundman KB. Heavy-section ADI: fatigue properties in the as-cast and austempered condition. AFS Trans 1991;111:563–70.
[11] Tayanç M, Aztekin K, Bayram A. The effect of matrix structure on the fatigue behavior of austempered ductile iron. Mater Des 2007;28:797–803.
[12] Toktaş G, Tayanç M, Toktaş A. Effect of matrix structure on the impact properties of an alloyed ductile iron. Mater Charact 2006;57:290–9.

[13] TS 138 EN 10002-1. Metallic materials – tensile testing: part 1. Methods of test (at ambient temperature); 1996.
[14] Hafız M. Mechanical properties of SG-iron with different matrix structure. J Mater Sci 2001;36:1293–300.
[15] Achary J. Tensile properties of austempered ductile iron under thermomechanical treatment. J Mater Eng Perform 2000;9:56–61.
[16] Trudel A, Gagne M. Effect of composition and heat treatment parameters on the characteristics of austempered ductile irons. Can Metall Quart 1997;36:289–98.
[17] Rao PP, Putatunda SK. Investigations on the fracture toughness of austempered ductile irons austenitized at different temperatures. Mater Sci Eng A 2003;349:136–49.
[18] Shanmugam P, Rao PP, Udupa KR, Venkataraman N. Effect of microstructure on the fatigue strength of an austempered ductile iron. J Mater Sci 1994;29:4933–40.
[19] Ductile iron data for design engineers. Rio Tinto Iron and Titanium Inc., Canada; 1990.
[20] Yescas-Gonzalez, Ph.D. Thesis, University of Cambridge, Department of Materials Science and Metallurgy; 2001.
[21] Eric O, Rajnovic D, Sidjanin L, Zec S, Jovanovic MT. An austempering study of ductile iron alloyed with copper. J Serb Chem Soc 2005;70:1015–22.
[22] Putatunda SK, Gadicherla PK. Influence of austenitizing temperature on fracture toughness of a low manganese austempered ductile iron (ADI) with ferritic as-cast structure. Mater Sci Eng A 1999;268:15–31.
[23] Putatunda SK, Gadicherla PK. Effect of austempering time on mechanical properties of a low manganese austempered ductile iron. J Mater Eng Perform 2000;9:193–203.
[24] Putatunda SK. Development of austempered ductile cast iron (ADI) with simultaneous high yield strength and fracture toughness by a novel two step austempering process. Mater Sci Eng A 2001;315:70–80.
[25] Rao PP, Putatunda SK. Investigation on the fracture toughness of austempered ductile iron alloyed with chromium. Mater Sci Eng A 2003;346:254–65.
[26] Bosnjak B, Radulovic B, Pop-Tonev K, Asanoviv V. Influence of microalloying and heat treatment on the kinetics of bainitic reaction in austempered ductile iron. J Mater Eng Perform 2001;10:203–11.
[27] Luo J, Harding RA, Bowen P. Evaluation of the fatigue behavior of ductile irons with various matrix structures. Metal Mater Trans A 2002;33:3719–30.
[28] Rundman KB. Heat treating of ductile irons. ASM Handbook, Heat treating, vol. 4. 10 ed. ASM International; 1991. p. 682.
[29] Lin CK, Lai PK, Shih TS. Influence of microstructure on the fatigue properties of austempered ductile irons – I. High-cycle fatigue. Int J Fatigue 1996;18:297–307.
[30] Lin CK, Chang CW. Influence of heat treatment on fatigue crack growth of austempered ductile iron. J Mater Sci 2002;37:709–16.
[31] Marrow TJ, Çetinel H. Short fatigue cracks in austempered ductile cast iron (ADI). Fatigue Fract Eng Mater Struct 2000;23:425–34.